

DOI: 10.1002/adma.200602085

# Electron and Hole Transport through Mesoporous $\text{TiO}_2$ Infiltrated with Spiro-MeOTAD\*\*

By Henry J. Snaith\* and Michael Grätzel

The solid-state dye-sensitized solar cell (SDSC) is a potential candidate to replace silicon photovoltaic technologies.<sup>[1]</sup> However, the current embodiment of the device is hampered because it only operates efficiently when the device thickness is significantly less than the light absorption depth of the composite. This fundamentally limits the maximum current attainable from incident sun light.<sup>[2]</sup> The necessity for the active layers to be thin has been thought to be due to incomplete filling of the  $\text{TiO}_2$  pores with the hole-transporter material (2,2',7,7'-tetrakis(*N,N*-di-*p*-methoxyphenyl-amine)-9,9'-spirobifluorene; Spiro-MeOTAD),<sup>[3]</sup> and the relatively low charge carrier mobility in the Spiro-MeOTAD,<sup>[4]</sup> as compared to crystalline  $\text{TiO}_2$ .<sup>[5,6]</sup> Here, we fabricate and test in-plane “hole-only” and “electron-only” devices and selectively measure the conductivity through the  $\text{TiO}_2$  and the Spiro-MeOTAD. We find that the hole conductivity through the composite is approximately three times higher than the electron conductivity. From the conductivity measurements under illumination (white light,  $100 \text{ mW cm}^{-2}$ ) we have estimated the hole and electron mobilities in the composite to be  $3 \times 10^{-4} \text{ cm}^2 \text{ V}^{-1} \text{ s}^{-1}$  and  $0.8 \times 10^{-4} \text{ cm}^2 \text{ V}^{-1} \text{ s}^{-1}$ , respectively. We observe, contrary to expectations, that the mobility in the  $\text{TiO}_2$  decreases as the illumination intensity is increased towards intensities comparable with full sunlight. We verify this observation by performing transient photocurrent measurements in complete solar cells at an equivalent potential to open-circuit. We find that the effective diffusion coefficient for electrons reduces considerably as the light intensity approaches solar illumination intensities, with the diffusion length becoming shorter than the film thickness. This highlights that poor electron transport in the mesoscopic  $\text{TiO}_2$  is a critical issue to be addressed to achieve further improvements in device performance.

The SDSC is composed of transparent conducting glass coated with a thin layer ( $2 \mu\text{m}$ ) of  $\text{TiO}_2$  nanoparticles ( $\sim 18 \text{ nm}$  diameter, 60 % porosity). The mesoporous  $\text{TiO}_2$  film

is coated with a monolayer of dye molecules, infiltrated with a hole transporting material, 2,2',7,7'-tetrakis(*N,N*-di-*p*-methoxyphenyl-amine)-9,9'-spirobifluorene (Spiro-MeOTAD), and capped with a gold counter electrode.<sup>[1]</sup> Light is absorbed in the dye molecules with subsequent electron transfer to the  $\text{TiO}_2$  and collection at the anode. The dye is regenerated by hole transfer to the HTM, with subsequent hole collection at the gold cathode.

The hole-only in-plane conductivity devices studied here are composed of an active layer identical to that in the SDSC, however electronic contact is only made on top to the Spiro-MeOTAD with gold electrodes defining a  $100 \mu\text{m}$  channel length. The electron-only devices are similar, however electronic contact is made selectively to the  $\text{TiO}_2$  nanoparticles on the underside of the film, with titanium electrodes defining an  $80 \mu\text{m}$  channel length. Figure 1 shows a schematic illustration of the device structures.

First, we need to verify that these devices truly exhibit hole-only and electron-only characteristics. This necessitates ohmic contacts with negligible resistance between the electrodes and their respective material, and blocking contacts between the

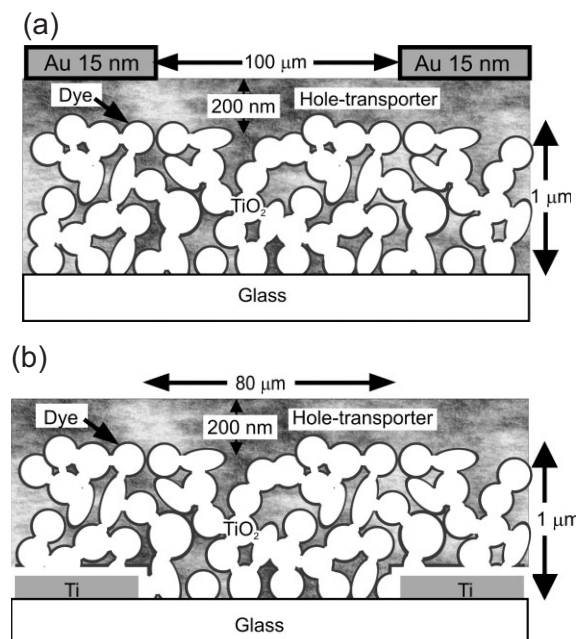


**Figure 1.** Schematic representation of the structure of the, a) hole-only, and b) electron only in-plane devices. The schematics are not to scale; the  $\text{TiO}_2$  nanoparticles are approximately 18 nm in diameter and the dye coverage is approximately one monolayer, other dimensions shown.

\* Dr. H. J. Snaith, Prof. M. Grätzel  
Institut de Chimie Physique, École Polytechnique Fédérale de Lausanne  
1015 Lausanne (Switzerland)  
E-mail: hjs36@cam.ac.uk

\*\* This work was funded by the MOLYCEL European project (OFES 03.0681-1). We thank Robin Humphry-Baker for valuable discussions and experimental assistance.

titanium and the Spiro-MeOTAD and between the gold and the  $\text{TiO}_2$ . The blocking between the gold and the  $\text{TiO}_2$  is facilitated by a 200 nm capping layer of Spiro-MeOTAD on top of the mesoporous film.<sup>[3]</sup> Furthermore, gold is known to form a Schottky barrier with  $\text{TiO}_2$  resulting in a poor electronic contact.<sup>[7]</sup> During the fabrication of the electron-only devices, a thermal layer of  $\text{TiO}_2$  will form on the titanium electrodes. We have found that a surface layer of titanium of approximately 80 nm thick is converted to  $\text{TiO}_2$ .<sup>[8]</sup> To verify that this blocks hole injection into the Spiro-MeOTAD we spin-coated a standard hole-transporter solution on top of the annealed electrodes (no mesoporous  $\text{TiO}_2$ ) and measured the current–voltage characteristics between the electrodes. There was negligible current measured, demonstrating a good blocking contact.

In Figure 2a we present the current–voltage characteristics under low light intensity through hole-only devices and

through electron-only devices where the  $\text{TiO}_2$  is infiltrated with Spiro-MeOTAD (with and without the addition of lithium salt). For the hole-only devices we observe approximately 2 orders of magnitude enhancement in current when the lithium salts are present in the Spiro-MeOTAD. For the electron-only device we observe an even more significant increase in current when the lithium salts are present in the surrounding matrix. We note that the dark conductivity of the “empty” dyed mesoporous  $\text{TiO}_2$  film was similar to that when infiltrated with pure Spiro-MeOTAD (no Li). When plotted on a linear axis all curves are straight lines, consistent with ohmic contacts between the respective electrodes and the charge transporting materials. By taking the resistance as the gradients of the curves we can estimate the conductivity ( $\sigma$ ) through the film (assuming negligible contact resistance, which has been verified by channel length variation). The conductivity is plotted against incident light illumination intensity in Figure 2b.

The conductivity of a material ( $\sigma$ ) is equal to the product  $n e \mu$ , where  $n$  is the charge density,  $e$  is the charge of an electron and  $\mu$  is the mobility. The enhancement in conductivity with increasing illumination intensity, observed for all devices, may be due to either increased charge density or enhanced mobility or a combination of the two. Since we are illuminating our devices, if we assume that the majority of the charges are photo-induced we can estimate the charge density in each film as a function of illumination intensity, and thus the mobility at each intensity can be extracted (see Experimental).<sup>[9]</sup> In Figure 3a the calculated mobility is plotted for the four different devices as a function of illumination intensity.

First, we consider the transport through the pristine Spiro-MeOTAD within the  $\text{TiO}_2$  network. From dark to full sun illumination intensity we observe almost a two order of magnitude enhancement in conductivity, with the conductivity scaling as  $I^{0.65}$  over a large intensity range. This corresponds to approximately a one order of magnitude enhancement in hole mobility. The calculated mobility for the Spiro-MeOTAD at low light intensity ( $\sim 4 \times 10^{-5} \text{ cm}^2 \text{ V}^{-1} \text{ s}^{-1}$ ) is approximately one order of magnitude less than that reported for solid films of pristine Spiro-MeOTAD ( $2 \times 10^{-4} \text{ cm}^2 \text{ V}^{-1} \text{ s}^{-1}$ ).<sup>[4]</sup> This is likely to be due to the disordered network of  $\text{TiO}_2$  nanoparticles around which the charges flow. However, once the charge density is enhanced, via increased illumination, the mobility becomes comparable with literature values, likely to be due to the filling of deeper energy “trap” sites. We have recently investigated the charge transport in Spiro-MeOTAD films with and without the addition of lithium salts.<sup>[10]</sup> We have postulated that the enhancement in mobility in Spiro-MeOTAD “doped” with lithium salts is primarily due to an increased disorder in the film and a broadening of the tail of the density-of-states. This would enable easier hopping between lower energy sites due to an overlapping of “trap” sites, similar to the influence of chemical p-dopant anions upon the charge transport in organic materials.<sup>[11]</sup> The hole mobility in the lithium salt doped Spiro-MeOTAD sample appears relatively insensitive to changes in charge density in the film. This is

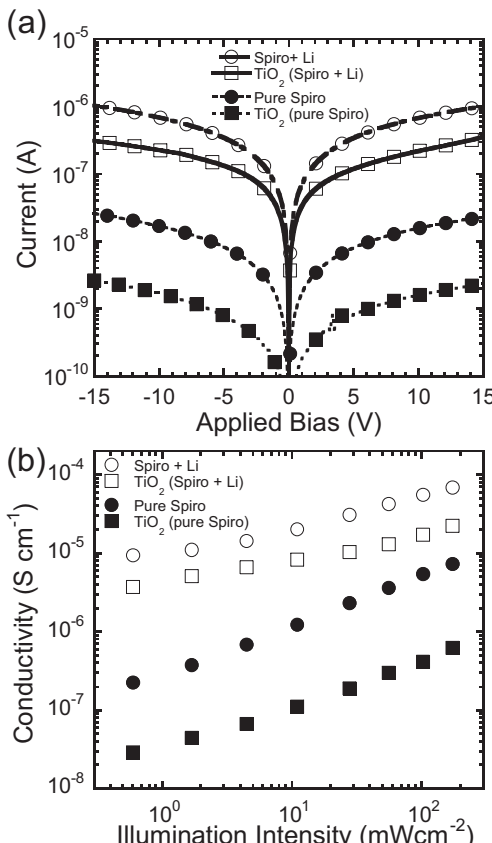


**Figure 2.** a) Current–voltage curves through “hole-only” and “electron-only” in-plane devices, measuring the electron transport through the  $\text{TiO}_2$  (squares), and the hole transport through the Spiro-MeOTAD (circles), under  $0.6 \text{ mWcm}^{-2}$  white light illumination, with the addition of (open symbols) and in the absence of lithium salts (solid symbols) in the Spiro-MeOTAD solution. b) The conductivity ( $\sigma$ ) through the films (calculated as  $\sigma = L/Rwt$ , where  $L$  is the channel length,  $w$  is the channel width,  $t$  is the film thickness and  $R$  is the film resistance calculated from the gradients of the curves) as a function of incident light intensity. We note that the dark conductivity of the “empty” dyed  $\text{TiO}_2$  mesoporous film was similar to that when infiltrated with pure Spiro-MeOTAD (no Li).

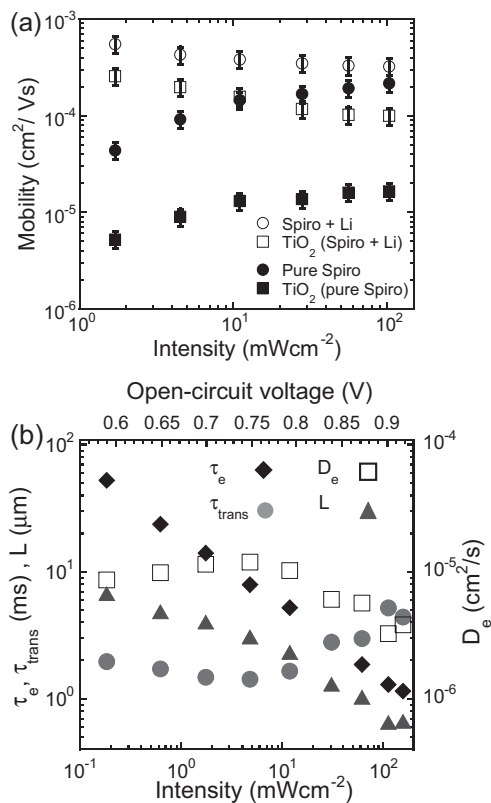


**Figure 3.** a) Charge carrier mobility versus light intensity calculated from the data in Figure 2b. The error bars are set at  $\pm 20\%$  due to our estimation of the charge generation efficiency. b) The Charge recombination lifetime and the electron transport lifetime measured in a  $2 \mu\text{m}$  thick solar cell (containing lithium salts) at potentials equivalent to open-circuit. Also shown are the effective diffusion coefficient and the diffusion length calculated from this data as a function of illumination intensity. The corresponding open-circuit voltage is shown on the top axis, though we note this is an approximate scale since there is a marginal difference in the position of the data points when plotting against  $V_{\text{oc}}$  or intensity on a log scale. We also note that the solar cells do not appear to be RC limited over the range of illumination intensities measured [10].

consistent with our proposed mechanism for mobility enhancement since the “smoothing” of the potential landscape has already enabled transport between sites which were previously acting as traps, thus negating any benefits of trap filling.

Considering the electron transport in the  $\text{TiO}_2$ , the most significant observation for this study is that the charge carrier mobility is significantly less than that through the Spiro-MeOTAD, at all illumination intensities. For  $\text{TiO}_2$  infiltrated with pure Spiro-MeOTAD the mobility increases at first but then becomes constant with increasing illumination intensity. The mobility through the  $\text{TiO}_2$  appears to be enhanced at all intensities when ions are present in the surrounding matrix. This may be due to improved matching between the dielectric constants of the  $\text{TiO}_2$  and its surrounding medium.<sup>[6]</sup> Alternatively, this may suggest that the inter-particle electron transfer is enhanced by the presence of the “charge-screening” medium. Unexpectedly, for the  $\text{TiO}_2$  infiltrated

with lithium salt containing Spiro-MeOTAD, we observe the mobility decrease as the illumination intensity is enhanced. This observation seems to be contrary to the multi-trapping (MT) model for electron transport, where transport in the  $\text{TiO}_2$  occurs via de-trapping of electrons from sub band-gap states into the conduction band (or mobility edge).<sup>[12]</sup> Thus, we expect the average mobility to constantly increase with increasing potential (charge density) within the device. If we draw a comparison to earlier work by Abayev et al.,<sup>[13]</sup> they measured the conductivity through a  $\text{TiO}_2$  mesoporous film in a similar set up to ours, however they employed a three electrode electrochemical cell in order to control the potential within the  $\text{TiO}_2$ , and they used gold source and drain electrodes. Abayev et al. observed an exponential increase in conductivity as the potential in the  $\text{TiO}_2$  was increased towards the conduction band. If the charge density also increased exponentially then this does not necessarily imply enhanced mobility. The gradient of the conductivity versus potential was also observed to constantly reduce from low to high potential,<sup>[13]</sup> possibly being consistent with our observations here of reducing mobility with increasing the potential within the  $\text{TiO}_2$ . We also note that gold is known to form a Schottky barrier with  $\text{TiO}_2$ ,<sup>[7]</sup> and thus a non-negligible potential varying contact resistance may exist, making interpretation of results using a gold electrode setup complicated.

At first sight, our measurements do appear to be at odds with a large quantity of experimental evidence which demonstrates that the effective electron diffusion coefficient in mesoporous  $\text{TiO}_2$ , generally measured in solar cells at short-circuit, increases with increasing illumination intensity.<sup>[14–25]</sup> However, in the in-plane devices studied here electronic contact is made exclusively to one material, thus the electronic situation is similar to that in a solar cell at open-circuit. Secondly, here we are measuring the conductivity through the  $\text{TiO}_2$  surrounded with hole-transporter and not an electrolyte. The ionic nature of an electrolyte may play a critical role in electron transport through mesoporous  $\text{TiO}_2$ .<sup>[26,27]</sup>

To verify that our results are consistent with transport in SDSCs, we have performed transient photocurrent and open-circuit voltage decay measurements, at an equivalent potential to open-circuit in complete SDSCs. A white-light bias is used to control the potential in the  $\text{TiO}_2$  and a low intensity pulsed square wave red light is superimposed. The decay of the perturbed signal is measured on an oscilloscope or through a fast source and measuring unit. The voltage perturbation is measured at open-circuit. Since no current is collected, the decay of the signal is purely due to charges recombining within the device and thus gives an estimate of the electron recombination lifetime ( $\tau_e$ ). For the current decay measurements a potential difference is applied across the device equivalent to the open-circuit voltage generated under the bias white light. In this instance charges are collected and recombine in the device simultaneously, thus the lifetime of the signal decay ( $\tau_{\text{signal}}$ ) is a combination of the electron transport lifetime ( $\tau_{\text{trans}}$ ) and  $\tau_e$  as  $1/\tau_{\text{signal}} = 1/\tau_e + 1/\tau_{\text{trans}}$ . Knowing the transport lifetime and the electron recombination lifetime the effective

electron diffusion coefficient ( $D_e$ ) can be estimated as,  $D_e = w^2/2.35 \tau_{trans}$ ,<sup>[28]</sup> where  $w$  is the film thickness, and the charge diffusion length ( $L$ ) can be estimated as,  $L = \sqrt{D_e \tau_e}$ .<sup>[29]</sup> These four parameters are plotted as a function of illumination intensity in Figure 3b.

The estimated charge recombination lifetime reduces considerably with increasing the illumination intensity. However, the estimated charge transport lifetime reduces marginally and then increases as the illumination intensity is increased. This results in an effective electron diffusion coefficient which reduces with increasing the light intensity above  $5 \text{ mW cm}^{-2}$ . The reduction in the effective diffusion coefficient with increasing illumination intensity is qualitatively in very good agreement with the in-plane conductivity measurements. To verify that the techniques are quantitatively comparable we can estimate the electron mobility from the diffusion coefficient using a modified version of the Nernst-Einstein relation, specifically applicable to mesoporous  $\text{TiO}_2$ ,  $\mu = e D / 2 k_B T$ .<sup>[30]</sup> Under illumination of  $50 \text{ mW cm}^{-2}$  the calculated  $D_e \sim 6 \times 10^{-6} \text{ cm}^2 \text{s}^{-1}$ , corresponding to a mobility of  $1.2 \times 10^{-4} \text{ cm}^2 \text{V}^{-1} \text{s}^{-1}$ . The estimated mobility from the in-plane electron-only device under the same illumination is approximately  $1.0 \times 10^{-4} \text{ cm}^2 \text{V}^{-1} \text{s}^{-1}$ , demonstrating remarkable consistency. These results are inconsistent with transport purely being governed by de-trapping of electrons as described by the multiple trapping model.<sup>[12]</sup> It is likely that a second mechanism which causes a reduction in the mobility with increasing charge density is also playing a critical role: This observation can not be due to the second order effects of the increasing electron-hole recombination rate constant at higher light intensities, since this will influence the electron diffusion length but not the electron diffusion coefficient. We postulate that it is a consequence of the electrostatic interaction of electrons in the spatially confined mesostructured  $\text{TiO}_2$ . In order to verify this and to elucidate the exact nature of the interactions and electrostatic influence, further experimental and theoretical investigations are necessary. However, if this is the case then this observed trend in transport may be very different in the solid-state device studied here as compared to  $\text{TiO}_2$  filled with an electrolyte, where charge screening and compensation is highly effective. This may explain why O'Regan et al. do not observe this trend in electron diffusion when measuring the transport in liquid electrolyte DSCs under conditions equivalent to open-circuit.<sup>[31]</sup>

The measurements here are performed at open-circuit, and the situation under the normal solar cell operating regime (maximum power point) may be very different.<sup>[32]</sup> Elsewhere we will present a full investigation into the transport and recombination under all working conditions, which yields further insight into the charge transport mechanisms in this class of materials. However, we note that we do find that the electron transport lifetime does decrease exponentially with increasing illumination intensity when measured in the low potential regime of short-circuit, consistent with previous studies on SDSCs.<sup>[14]</sup>

We have calculated that the electron diffusion length reduces from approximately  $6 \mu\text{m}$  at low light levels to  $0.6 \mu\text{m}$  under standard solar illumination intensities ( $100 \text{ mW cm}^{-2}$ ). This is less than the device thickness ( $2 \mu\text{m}$ ), illustrating that loss to device performance near open-circuit will be occurring due to the slow diffusion of electrons in the mesoporous  $\text{TiO}_2$  film. The conductivity of mesoporous  $\text{TiO}_2$  has been observed to be inversely proportional to the "roughness" of the film (i.e., the larger the particles the faster the transport).<sup>[33]</sup> This appears to pose a dilemma, since the light absorption and thus charge generation increase with the surface area. However, with the advent of new "high extinction coefficient" dyes, surface area is becoming less of a critical issue for light harvesting.<sup>[34,35]</sup> As a means to improve and further probe the charge transport in our devices we are currently investigating a range of sizes of  $\text{TiO}_2$  nanoparticles.

In summary, from in-plane conductivity measurements we have demonstrated that the hole transport within the  $\text{TiO}_2$ :Spiro-MeOTAD composite is faster than the electron transport, with calculated mobilities of  $3.2 \times 10^{-4} \text{ cm}^2 \text{V}^{-1} \text{s}^{-1}$  and  $1.0 \times 10^{-4} \text{ cm}^2 \text{V}^{-1} \text{s}^{-1}$ , respectively, under  $100 \text{ mW cm}^{-2}$  white light illumination. From transient photocurrent measurements, performed at an equivalent potential to open-circuit, we observe the effective electron diffusion coefficient reduce as the illumination intensity is increased. This results in a diffusion length which reduces considerably with increasing illumination intensity, becoming less than the film thickness under moderate illumination intensities. This demonstrates that a key issue to be addressed in order to further enhance the performance of the solid-state dye-sensitized solar cell is the "poor" electron transport in mesoporous  $\text{TiO}_2$ .

## Experimental

The "hole-only" devices were fabricated as follows: A pre-cleaned glass slide was coated with a mesoporous  $\text{TiO}_2$  film to give a dry film thickness of approximately  $1 \mu\text{m}$ . These films were annealed, treated with an aqueous solution of  $\text{TiCl}_4$ , dyed and infiltrated with hole-transporter as previously described [36]. Lithium bis(trifluoromethylsulfonyl) amine (Li-TFSI) was optionally added to the Spiro-MeOTAD solution prior to spin-coating at a concentration of 12% molar ratio to Spiro-MeOTAD. The dye used was a ruthenium bi-pyridyl complex termed K68 (which will be described elsewhere). The devices were capped with gold electrodes with  $100 \mu\text{m}$  channel length defined by shadow mask evaporation. The "electron-only" devices were fabricated in a similar manner. However, before the application of the mesoporous  $\text{TiO}_2$  film, titanium electrodes were sputtered upon the glass slide with an  $80 \mu\text{m}$  channel length defined by a shadow mask, and measured under an optical microscope. Gold top electrodes were not employed in this instance. The solar cells were fabricated as previously described [36], however no chemical p-dopants were added to the Spiro-MeOTAD. Transient open-circuit voltage and current decay measurements were performed by a similar method to that used by O'Regan et al. [37,38]: Here, a white light bias was generated from an array of diodes (Lumiled Model LXHL-NWE8 whitestar) with red light pulsed diodes (LXHL-ND98 redstar, 0.2 s square pulse width, 100 ns rise and fall time) as the perturbation source, controlled by a fast solid state switch. The voltage dynamics were recorded on a P.C.

interfaced Keithley 2400 sourcemeter with a 500  $\mu$ s sampling time and a 5  $\mu$ s response time to an abrupt change in load. The perturbation light source was set to a suitably low level that the voltage decay kinetics were mono-exponential. This enabled the charge recombination lifetime to be obtained directly from the inverse of the exponential decay rate of the voltage decay. Small perturbation transient photocurrent measurements were performed in a similar manner to the open-circuit voltage decay measurement. However, the signal was recorded through a low impedance port (50  $\Omega$ ) on an oscilloscope with the Keithley sourcemeter, in series with the solar cell and the oscilloscope, holding a potential difference across the device equivalent to the open-circuit voltage under the bias white light illumination. The same white light diode source was used for the conductivity measurements. Since only the Spiro-MeOTAD or the TiO<sub>2</sub> are electronically contacted in the in-plane conductivity devices, the situation in the active layer is similar to that in a photovoltaic diode at open-circuit. In order to estimate the charge lifetime ( $\tau_e$ ) in the in plane devices, we fabricated solid-state dye-sensitized solar cells (sandwich cell configuration) [1] incorporating identical active layers to those in the in-plane devices. The charge lifetime as a function of illumination intensity was then estimated by employing open-circuit voltage decay measurements. Assuming charge generation efficiency from absorbed photons of 0.8 [39], the charge generation rate ( $G$ ) as a function of illumination intensity was estimated by taking the overlap integral of the light source with the dye absorption. Thus, assuming that the dark charge density  $\ll$  the photo-induced charge density, the charge density ( $n$ ) was calculated from the steady state rate equation,  $dn/dt = G - n/\tau = 0$  and the mobility ( $\mu$ ) from,  $\mu = \sigma/n e$  [9].

Received: September 13, 2006

Revised: May 22, 2007

Published online: October 16, 2007

- [1] U. Bach, D. Lupo, P. Comte, J. E. Moser, F. Weissert, J. Salbeck, H. Spreitzer, M. Grätzel, *Nature* **1998**, 395, 583.
- [2] L. Schmidt-Mende, S. M. Zakeeruddin, M. Grätzel, *Appl. Phys. Lett.* **2005**, 86, 013504.
- [3] L. Schmidt-Mende, M. Grätzel, *Thin Solid Films* **2006**, 500, 296.
- [4] D. Poplavskyy, J. Nelson, *J. Appl. Phys.* **2003**, 93, 341.
- [5] G. Kron, T. Egerter, J. H. Werner, U. Rau, *J. Phys. Chem. B* **2003**, 107, 3556.
- [6] E. Hendry, M. Koeberg, B. O'Regan, M. Bonn, *Nano Lett.* **2006**, 6, 755.
- [7] G. Kron, U. Rau, J. H. Werner, *J. Phys. Chem. B* **2003**, 107, 13258.
- [8] TiO<sub>2</sub> is transparent to visible light and it is easily verified when a titanium film has been completely oxidized. By sputtering films of various thickness, and exposing these films to the standard device fabrication processes, we have found that the metal becomes completely oxidized when the film is thinner than approximately 80 nm.
- [9] H. J. Snaith, M. Grätzel, *Phys. Rev. Lett.* **2006**, 98, 177402.
- [10] The solar cell becomes RC limited when the "in-plane" series resistance through the FTO becomes comparable with the "out-of-plane" series resistance through the TiO<sub>2</sub>. From the conductivity measurements we calculate the series resistance at the highest light intensity of 100 mW cm<sup>-2</sup> to be approximately 65  $\Omega$ . The series resistance through the FTO in our device configuration is approximately 8  $\Omega$ . So the cell is approaching but still some way off RC limitations at the highest light intensities.
- [11] H. J. Snaith, M. Grätzel, *Appl. Phys. Lett.* **2006**, 89, 262114.
- [12] V. I. Arkhipov, P. Heremans, E. V. Emelianova, H. Bassler, *Phys. Rev. B* **2005**, 71, 045214.
- [13] J. Bisquert, *J. Phys. Chem. B* **2004**, 108, 2323.
- [14] I. Abayev, A. Zaban, F. Fabregat-Santiago, J. Bisquert, *Phys. Status Solidi A* **2003**, 196, R4.
- [15] J. Kruger, R. Plass, M. Grätzel, P. J. Cameron, L. M. Peter, *J. Phys. Chem. B* **2003**, 107, 7536.
- [16] S. A. Haque, Y. Tachibana, R. L. Willis, J. E. Moser, M. Grätzel, D. R. Klug, J. R. Durrant, *J. Phys. Chem. B* **2000**, 104, 538.
- [17] N. Kopidakis, K. D. Benkstein, J. van de Lagemaat, A. J. Frank, *J. Phys. Chem. B* **2003**, 107, 11307.
- [18] J. Nelson, S. A. Haque, D. R. Klug, J. R. Durrant, *Phys. Rev. B* **2001**, 6320, 205321.
- [19] F. Cao, G. Oskam, G. J. Meyer, P. C. Searson, *J. Phys. Chem.* **1996**, 100, 17021.
- [20] P. E. deJongh, D. Vanmaekelbergh, *Phys. Rev. Lett.* **1996**, 77, 3427.
- [21] L. Dloczik, O. Illeperuma, I. Lauermann, L. M. Peter, E. A. Ponomarev, G. Redmond, N. J. Shaw, I. Uhlendorf, *J. Phys. Chem. B* **1997**, 101, 10281.
- [22] A. Kambili, A. B. Walker, F. L. Qiu, A. C. Fisher, A. D. Savin, L. M. Peter, *Phys. E* **2002**, 14, 203.
- [23] N. Kopidakis, E. A. Schiff, N. G. Park, J. van de Lagemaat, A. J. Frank, *J. Phys. Chem. B* **2000**, 104, 3930.
- [24] K. Lobato, L. M. Peter, U. Wurfel, *J. Phys. Chem. B* **2006**, 110, 16201.
- [25] K. Schwarzburg, F. Willig, *Appl. Phys. Lett.* **1991**, 58, 2520.
- [26] J. van de Lagemaat, A. J. Frank, *J. Phys. Chem. B* **2000**, 104, 4292.
- [27] S. Kambe, S. Nakade, T. Kitamura, Y. Wada, S. Yanagida, *J. Phys. Chem. B* **2002**, 106, 2967.
- [28] S. Nakade, S. Kambe, T. Kitamura, Y. Wada, S. Yanagida, *J. Phys. Chem. B* **2001**, 105, 9150.
- [29] J. van de Lagemaat, A. J. Frank, *J. Phys. Chem. B* **2001**, 105, 11194.
- [30] L. M. Peter, K. G. U. Wijayanta, *Electrochim. Commun.* **1999**, 1, 576.
- [31] J. van de Lagemaat, N. Kopidakis, N. R. Neale, A. J. Frank, *Phys. Rev. B* **2005**, 71, 035304.
- [32] B. C. O'Regan, K. Bakker, J. Kroese, H. Smit, P. Sommeling, J. R. Durrant, *J. Phys. Chem. B* **2006**, 110, 17155.
- [33] J. Nissfolk, K. Fredin, A. Hagfeldt, G. Boschloo, *J. Phys. Chem. B* **2006**, 110, 17715.
- [34] N. Kopidakis, N. R. Neale, K. Zhu, J. van de Lagemaat, A. J. Frank, *Appl. Phys. Lett.* **2005**, 87, 202106.
- [35] L. Schmidt-Mende, U. Bach, R. Humphry-Baker, T. Horiuchi, H. Miura, S. Ito, S. Uchida, M. Grätzel, *Adv. Mater.* **2005**, 17, 813.
- [36] S. Ito, S. M. Zakeeruddin, R. Humphry-Baker, P. Liska, R. Charvet, P. Comte, M. K. Nazeeruddin, P. Pechy, M. Takata, H. Miura, S. Uchida, M. Grätzel, *Adv. Mater.* **2006**, 18, 1202.
- [37] H. J. Snaith, L. Schmidt-Mende, M. Chiesa, M. Grätzel, *Phys. Rev. B* **2006**, 74, 045306.
- [38] B. C. O'Regan, J. R. Durrant, *J. Phys. Chem. B* **2006**, 110, 8544.
- [39] B. C. O'Regan, F. Lenzmann, *J. Phys. Chem. B* **2004**, 108, 4342.
- [40] J. E. Kroese, N. Hirata, S. Koops, M. K. Nazeeruddin, L. Schmidt-Mende, M. Grätzel, J. R. Durrant, *J. Am. Chem. Soc.* **2006**, 128, 16376.